changing proton by a more restricted trajectory perhaps because of the steric effects described above. The activation enthalpies we observe and the electronic explanation we offer for the different rate of exchange of the glycine protons is consistent with a recent neutron diffraction study of a related system.[18] In the (salicylideneglycinato)copper(II) complex, it was observed that the glycine chelate ring was distorted and the proton had dihedral angles of -32.9 and $77.9°$ with the plane of the salicyl aromatic ring. It was observed that the proton at the higher angle had a C–H bond length more than 3σ longer than the proton at the lower angle. The longer bond length is consistent with a reduced ΔH^* for exchange, such as we observe.

A concluding point concerns the magnitude of ΔH^* for the more rapidly exchanging proton. In an enzyme, the base is part of the active site. This enables ΔS^* to be close to zero. If ΔS^* were zero in our system, one may calculate that the rate constant would be 300 L mol^{-1} s^{-1}. This approaches the rates observed for enzyme-catalyzed reactions.

Supplementary Material Available: Listings of crystal data and structure refinement parameters, least-squares planes, and anisotropic thermal parameters (2 pages); a listing of observed and calculated structure factors (8 pages). Ordering information is given on any current masthead page.

(18) Bkouche-Waksman, I.; Barke, J. M.; Kvick, A. *Acta Crystallogr., Sect. B* **1988**, *B44*, 595.

A New Type of Divalent Metal Nucleosidate Complex: Crystal Structure of *trans*-Tetraaquobis(xanthosinato)zinc(II) Dihydrate

Miguel Quirós,[†] Juan M. Salas,[*,†] M. Purificación Sánchez,[†] Juan R. Alabart,[‡] and René Faure[§]

Several complexes of divalent transition metals with the anionic form of the purine nucleosides guanosine, inosine, and xanthosine have been isolated and characterized by thermal and spectroscopic techniques and magnetic measurements. The complexes have the general formula $[M(Nuc)_2(H_2O)_4]\cdot nH_2O$ (except the cadmium complex, which has the formula $[Cd(Xao)_2(H_2O)_2]\cdot 5H_2O$). The coordinated and uncoordinated water molecules are clearly identified by TG and DSC diagrams. The octahedral coordination for Mn, Co, Ni, and Cu is supported by the magnetic measurements. NMR data for cadmium xanthosinate indicate coordination through N3. The crystal structure of $trans$-$[Zn(Xao)_2(H_2O)_4]\cdot 2H_2O$ has been solved by X-ray diffraction. This is the first time that the structure of a xanthosine complex has been described and also the first description of the structure of a purine nucleoside complex with a divalent metal of the first transition series. The N7-coordinated xanthosinate is located at the apex of the octahedral complex. The structure reveals an interesting hydrogen-bonding scheme and unusual sugar conformations.

Introduction

The interaction of metal ions with nucleic acid derivatives is of considerable interest due to the biological importance of such compounds. The research carried out can be classified according to the complexity of the nucleic acid fragments, i.e. complexes with heterocyclic bases, nucleosides, nucleotides, polynucleotides, and nucleic acids themselves. The first case (bases) and the third case (nucleotides) have been studied much more than the second one (nucleosides), probably due to the fact that nucleoside complexes are generally obtained in the form of polymeric and colloidal species and are difficult to crystallize. More than 80 references to crystal structures of nucleotide–metal complexes exist compared to only 14 for pyrimidine and purine nucleoside–metal complexes: ($[Pt(en)(Guo)_2]Cl_{1.5}I_{0.5}\cdot 2H_2O$,[1] $[Co(acac)_2(NO_2)(dAdo)]$,[2] cis-$[Pt(NH_3)_2(Guo)_2]Cl_{1.5}(ClO_4)_{0.5}\cdot 7H_2O$,[3] $catena$-$[Hg(\mu$-Cl)Cl(Guo)]$,[4] $[Pt(dien)(Ino)](NO_3)_2$,[5] $[Pt(dien)(Guo)](ClO_4)_2$,[6] $[Pd(dien)(Guo)](ClO_4)_2$,[7] $[(CH_3Hg)_2(\mu$-Ino-$N1,N7)](ClO_4)$,[8] $[PtCl(en)(AraCyt)]Cl$,[9] $[CH_3Hg(Thd)]$,[10] $[Cu(GlyGly)(Cyd)]$,[11] $catena$-$[Hg(\mu Br)Br(Guo)]$,[12] $trans$-$[Pd(Ino)_2Cl_2]\cdot 5H_2O$, and $trans$-$[Pd(Ino)_2Br_2]\cdot 3H_2O$[13] where Guo = guanosine, dAdo = 2′-deoxyadenosine, Ino = inosine, AraCyt = 9-β-D-arabinofuranosylcytosine, Thd = thymidine, Cyd = cytidine, en = ethylenediamine, acac = acetylacetonato, dien = diethylenetri-

amine, and GlyGly = glycylglycinato).

Work on solid-phase studies of nucleoside–metal complexes has usually been focused on Pt(II),[1,3,5,6,14–18] Pd(II),[7,13,19,20] and Hg-

* To whom correspondence should be addressed.
† Universidad de Granada.
‡ Universidad de Barcelona.
§ Université Claude Bernard.

(1) Gellert, R. W.; Bau, R. *J. Am. Chem. Soc.* **1975**, *97*, 7379.
(2) Sorrel, T.; Epps, C. A.; Kistenmacher, T. J.; Marzilli, L. G. *J. Am. Chem. Soc.* **1977**, *99*, 2173.
(3) Cramer, R. E.; Dahlstrom, P. L.; Seu, M. J. T.; Norton, T.; Kashiwagi, M. *Inorg. Chem.* **1980**, *19*, 148.
(4) Authier-Martin, M.; Hubert, J.; Rivest, R.; Beauchamp, A. L. *Acta Crystallogr.* **1978**, *B34*, 273.
(5) Melanson, R.; Rochon, F. D. *Acta Crystallogr.* **1978**, *B34*, 3594.
(6) Melanson, R.; Rochon, F. D. *Can. J. Chem.* **1979**, *57*, 57.
(7) Rochon, F. D.; Kong, P. C.; Coulombe, B.; Melanson, R. *Can. J. Chem.* **1980**, *58*, 381.
(8) Bélanger-Gariepy, F.; Beauchamp, A. L. *Cryst. Struct. Commun.* **1982**, *11*, 991.
(9) Neidle, S.; Taylor, G. L.; Robins, A. B. *Acta Crystallogr.* **1978**, *B34*, 1838.
(10) Guay, F.; Beauchamp, A. L. *Can. J. Chem.* **1985**, *63*, 3456.
(11) Szalda, D. J.; Marzilli, L. G.; Kistenmacher, T. J. *Biochem. Biophys. Res. Commun.* **1975**, *63*, 601.
(12) Quirós, M.; Salas, J. M.; Sánchez, M. P.; Faure, R. *An. Quím.* **1990**, *86*, 518.
(13) Quirós, M.; Salas, J. M.; Sánchez, M. P.; Solans, X.; Beauchamp, A. L. *Can. J. Chem.*, submitted for publication.
(14) Hadjiliadis, N.; Theophanides, T. *Inorg. Chim. Acta* **1976**, *16*, 67.
(15) Hadjiliadis, N.; Theophanides, T. *Inorg. Chim. Acta* **1976**, *16*, 77.
(16) Kong, P. C.; Theophanides, T. *Inorg. Chem.* **1974**, *13*, 1167.
(17) Gullotti, M.; Pacchioni, G.; Pasini, A.; Ugo, R. *Inorg. Chem.* **1982**, *21*, 2006.
(18) Kasselouri, S.; Garoufis, A.; Hadjiliadis, N. *Inorg. Chim. Acta* **1987**, *135*, L23.

(II).[4,8,12,21,22] Only a few works referring to first-row transition metals[23,24] are available.

The reaction of purine nucleosides with divalent transition metals in basic media usually yields basic nonstoichiometric salts, which are difficult to isolate and characterize.[25,26] Nevertheless, we have been able to isolate a novel series of compounds, with the general formula $[M(Nuc)_2(H_2O)_4] \cdot nH_2O$, where Nuc represents the nucleoside anions inosinate (Ino), guanosinate (Guo), and xanthosinate (Xao) and M = Mn, Co, Ni, Cu, Zn, and Cd (the formula for the latter is $[Cd(Xao)_2(H_2O)_2] \cdot 5H_2O$). These compounds have been characterized using spectroscopic and magnetic measurements. The crystal structure of $[Zn(Xao)_2(H_2O)_4] \cdot 2H_2O$ is described. This is the first time that the structure of a xanthosine complex has been described and also the first description of the structure of a purine nucleoside complex with a divalent metal of the first transition series.

Experimental Section.

Materials. Guanosine and inosine came from Sigma and xanthosine from Aldrich Chemical and were used without further purification. Sodium inosinate $(Na(Ino) \cdot 2.5H_2O)$ was synthesized as indicated by Suzuki et al.[27]

Synthesis of Tetraaquobis(xanthosinato)manganese(II) Trihydrate (MnXao). Xanthosine (0.3 g, 0.94 mmol) was dissolved in water (50 mL). $MnCO_3$ (0.1 g, 0.87 mmol) was then added and the mixture stirred at approximately 70 °C for $^1/_2$ h. The nonreacted manganese carbonate was filtered off before cooling the solution. After several days of slow evaporation in air, the product appears as white prismatic crystals.

Anal. Calcd for $MnC_{20}N_8H_{36}O_{19}$: C, 32.50; H, 4.48; N, 15.82. Found: C, 32.11; H, 4.82; N, 14.98. Infrared bands in the 1800–1400-cm^{-1} range: 1680, 1645, 1602, 1567 cm^{-1}.

Synthesis of Tetraaquobis(inosinato)cobalt(II) Trihydrate (CoIno). Sodium inosinate (0.3 g, 1.03 mmol) and cobalt nitrate hexahydrate (0.13 g, 0.57 mmol) were dissolved separately in a small amount of boiling water. The two solutions were mixed, and on cooling, a pink powder was obtained, which was then recrystallized in water.

Anal. Calcd for $CoC_{20}N_8H_{36}O_{17}$: C, 32.68; H, 4.86; N, 15.25. Found: C, 33.36; H, 5.00; N, 15.57. IR bands: 1610, 1556, 1476 cm^{-1}.

Synthesis of Tetraaquobis(xanthosinato)cobalt(II) Trihydrate (CoXao). Cobalt carbonate (0.06 g, 0.45 mmol) was stirred for 5 h with a solution of xanthosine (0.3 g, 0.94 mmol) in water (50 mL) at 70 °C. When the solution was cooled, pale pink, laminate crystals were formed.

Anal. Calcd for $CoC_{20}N_8H_{36}O_{19}$: C, 31.85; H, 5.04; N, 15.14. Found: C, 31.94; H, 4.79; N, 14.91. IR bands: 1672, 1645, 1592, 1526, 1465 cm^{-1}.

Synthesis of Tetraaquobis(guanosinato)nickel(II) Dihydrate (NiGuo). Guanosine (0.3 g, 1.06 mmol), $Ni(NO_3)_2 \cdot 6H_2O$ (0.145 g, 0.50 mmol) and KOH (0.2 g, 3.57 mmol) were dissolved in NH_3 (1 M, 30 mL). The solution was kept at room temperature for several days while the excess ammonia evaporated off. The product appeared then as a pale blue powder.

Anal. Calcd for $NiC_{20}N_{10}H_{36}O_{16}$: C, 32.64; H, 4.92; N, 18.35. Found: C, 32.83; H, 4.92; N, 19.15. IR bands: 1692, 1630, 1613, 1585, 1453 cm^{-1}.

Synthesis of Tetraaquobis(inosinato)nickel(II) Trihydrate (NiIno). Inosine (0.3 g, 1.12 mmol) and nickel nitrate hexahydrate (0.16 g, 0.55 mmol) were dissolved in NH_3 (1 M, 30 mL). The result after a few days was a green powder, which was filtered off and on analysis turned out to be a basic salt. A second product was obtained from the mother liquor a few days later in the form of a pale blue powder, the formula for which is $[Ni(Ino)_2(H_2O)_4] \cdot 3H_2O$.

Anal. Calcd for $NiC_{20}N_8H_{36}O_{17}$: C, 33.30; H, 5.00; N, 15.55. Found: C, 33.37; H, 5.01; N, 15.57. IR bands: 1606, 1555, 1479 cm^{-1}.

Table I. Crystal Data for *trans*-$[Zn(Xao)_2(H_2O)_4] \cdot 2H_2O$

cryst habit and color	colorless plate
formula	$ZnC_{20}N_8H_{34}O_{18}$
cryst syst	triclinic
space group	$P1$
cell params at 293 K	
a, Å	8.065 (1)
b, Å	8.502 (1)
c, Å	11.066 (1)
α, deg	81.52 (1)
β, deg	84.67 (1)
γ, deg	82.73 (1)
V, Å^3	741.9 (2)
Z	1
D_{calc}, g·cm^{-3}	1.66
mol wt	739.9
cryst dimens, mm	0.10 × 0.35 × 0.50
scan type	$\omega = 5\theta/3$
2θ range, deg	2–70
no. of total data measd	6501
no. of obsd data measd	4556
criterion for observn	$I > 3\sigma(I)$
$F(000)$	384
$\lambda(Mo\ K\alpha)$, Å	0.7107
$\mu(Mo\ K\alpha)$, cm^{-1}	9.5
R	0.056
R_ω	0.075

Synthesis of Tetraaquobis(xanthosinato)nickel(II) Hexahydrate (NiXao). The mode of synthesis was the same as for NiIno but with xanthosine (0.3 g, 0.94 mmol) used instead of inosine. The product was also obtained via the reaction of xanthosine with nickel carbonate, but in this case it crystallized together with free xanthosine.

Anal. Calcd for $NiC_{20}N_8H_{42}O_{22}$: C, 29.85; H, 4.87; N, 13.82. Found: C, 29.81; H, 5.22; N, 13.91. IR bands: 1671 (wide), 1590, 1564 cm^{-1}.

Synthesis of Tetraaquobis(xanthosinato)copper(II) Tetrahydrate (CuXao). Basic copper carbonate (0.1 g, 0.45 mmol) was treated with a solution of xanthosine (0.3 g, 0.94 mmol) in water at ≈70 °C for about 3 h. The warm solution was then filtered to eliminate any unreacted copper carbonate and the basic salt formed in the process. The resulting solution was left to evaporate at room temperature and a few days later a mixture of green needles and white prismatic crystals, large enough to be separated with the aid of a lens, appeared. The white crystals were xanthosine, and the green ones were CuXao.

Anal. Calcd for $CuC_{20}N_8H_{38}O_{20}$: C, 30.48; H, 4.18; N, 13.72. Found: C, 31.01; H, 4.91; N, 14.48. IR bands: 1687, 1660, 1610, 1579 cm^{-1}.

Synthesis of Tetraaquobis(xanthosinato)zinc(II) Dihydrate (ZnXao). Basic zinc carbonate (0.2 g, 0.36 mmol) was stirred for 3 h in a solution of xanthosine (0.3 g, 0.94 mmol) in warm water. The excess carbonate was then filtered off and the solution was kept at room temperature. Then, 48 h later, white prismatic crystals of xanthosine appeared and were filtered off. When the volume of the mother liquor decreased to a few millilitres, the product appeared as white laminae.

Anal. Calcd for $ZnC_{20}N_8H_{34}O_{18}$: C, 32.18; H, 4.65; N, 15.42. Found: C, 32.44; H, 4.59; N, 15.14. IR bands: 1669 (wide), 1588 cm^{-1}.

Synthesis of Diaquobis(xanthosinato)cadmium(II) Pentahydrate (CdXao). NaOH (0.05 N) was added drop by drop to a cold suspension of xanthosine in water (20 mL) and stirred continuously until the nucleoside was completely dissolved. $CdCl_2 \cdot 2.5H_2O$ (0.11 g, 0.48 mmol) was then added and the solution filtered to eliminate the generated cadmium hydroxide. The product was obtained from the mother liquor as a white powder 48 h later.

Anal. Calcd for $CdC_{20}N_8H_{36}O_{19}$: C, 29.21; H, 4.43; N, 13.53. Found: C, 29.82; H, 4.47; N, 13.92. IR bands: 1680, 1610, 1550, 1529 cm^{-1}.

Instrumentation and Analysis. Elemental analyses were made by the Technical Services of the University of Granada. IR spectra were obtained with a Perkin-Elmer 983G spectrophotometer, using a KBr disk as dispersant. ^1H and ^{13}C NMR spectra were obtained in DMSO-d_6 solution with a Bruker AM300 NMR spectrometer (TMS as reference). TG and DSC curves were carried out on a Mettler TA-3000 system in pure air (flow rate 100 mL·min^{-1}).

Magnetic Measurements. Magnetic susceptibility measurements were carried out on powdered samples on a Faraday type microbalance in the 13–300 K temperature range in a magnetic field of ca. 2500 G for the Co(II) and Mn(II) derivatives, ca. 4500 G for the nickel derivatives and ca. 6500 G for the Cu(II) ones. A commercial closed-cycle helium-gas

(19) Pneumatikakis, G.; Hadjiliadis, N.; Theophanides, T. *Inorg. Chem.* **1978**, *17*, 915.

(20) Pneumatikakis, G. *Polyhedron* **1984**, *3*, 9.

(21) Buncel, E.; Norris, A. R.; Racz, W. J.; Taylor, S. E. *Inorg. Chem.* **1981**, *20*, 98.

(22) Buncel, E.; Hunter, B. K.; Kumar, R.; Norris, A. R. *J. Inorg. Biochem.* **1984**, *20*, 171.

(23) Beringhelli, F.; Freni, M.; Morazzoni, F.; Romiti, P.; Servida, R. *Spectrochim. Acta* **1981**, *37A*, 763.

(24) Mikulski, C. M.; Minutella, R.; De Franco, N.; Borges, G.; Karayannis, N. M. *Inorg. Chim. Acta* **1986**, *123*, 105.

(25) Nelson, H. C.; Villa, J. F. *Inorg. Chem.* **1979**, *18*, 1725.

(26) Nelson, H. C.; Villa, J. F. *J. Inorg. Nucl. Chem.* **1979**, *41*, 1643.

(27) Suzuki, Y.; Toki, T. *Bull. Chem. Soc. Jpn.* **1974**, *47*, 2556.

Table II. Atomic Coordinates (*10^4) and Isotropic Equivalent Factors

atom	x	y	z	B, Å^2
Zn	0	0	0	1.8
N1A	3327 (6)	−5460 (6)	−875 (5)	1.9
C2A	2656 (8)	−6318 (7)	−1653 (6)	1.7
O2A	3546 (7)	−7649 (6)	−1853 (5)	2.6
N3A	1199 (7)	−5814 (6)	−2121 (5)	1.8
C4A	508 (7)	−4430 (7)	−1745 (6)	1.6
C5A	1130 (8)	−3498 (7)	−1040 (6)	1.9
C6A	2670 (7)	−3981 (6)	−556 (5)	1.5
O6A	3494 (6)	−3264 (6)	33 (5)	2.8
N7A	−62 (7)	−2071 (6)	−917 (6)	2.2
C8A	−1281 (8)	−2221 (8)	−1603 (6)	2.2
N9A	−1011 (7)	−3643 (6)	−2121 (5)	1.8
C1′A	−1953 (9)	−4216 (9)	−2961 (6)	2.3
O1′A	−1177 (7)	−3931 (7)	−4159 (5)	2.8
C2′A	−3770 (8)	−3412 (10)	−3043 (7)	2.5
O2′A	−4656 (7)	−4616 (8)	−3404 (7)	3.9
C3′A	−3605 (9)	−2051 (9)	−4065 (7)	2.3
O3′A	−5071 (7)	−1667 (8)	−4742 (6)	3.4
C4′A	−2089 (11)	−2644 (12)	−4912 (8)	3.1
C5′A	−966 (13)	−1438 (16)	−5493 (13)	5.6
O5′A	−500 (12)	−578 (14)	−4584 (13)	7.7
N1B	−3427 (7)	5438 (7)	873 (5)	2.0
C2B	−2730 (7)	6355 (7)	1601 (6)	1.8
O2B	−3489 (6)	7633 (6)	1834 (5)	2.4
N3B	−1226 (7)	5805 (6)	2066 (5)	2.0
C4B	−489 (7)	4387 (7)	1730 (6)	1.5
C5B	−1069 (7)	3449 (6)	969 (5)	1.4
C6B	−2730 (9)	4012 (8)	520 (7)	2.3
O6B	−3474 (6)	3329 (6)	−151 (5)	3.0
N7B	23 (6)	2147 (6)	867 (5)	1.7
C8B	1256 (7)	2262 (7)	1511 (5)	1.6
N9B	1003 (6)	3596 (6)	2048 (5)	1.7
C1′B	1956 (7)	4062 (7)	3006 (6)	1.7
O1′B	3648 (6)	3811 (7)	2673 (5)	2.3
C2′B	1725 (8)	3036 (8)	4232 (6)	2.0
O2′B	138 (7)	3288 (7)	4852 (5)	3.0
C3′B	3201 (8)	3511 (9)	4858 (6)	2.2
O3′B	2692 (7)	4972 (7)	5296 (5)	3.2
C4′B	4519 (8)	3723 (9)	3771 (6)	2.0
C5′B	5901 (9)	2330 (10)	3729 (7)	2.8
O5′B	7011 (7)	2280 (8)	4667 (6)	3.4
OW1	2641 (6)	−116 (6)	−203 (6)	2.8
OW2	−2596 (6)	95 (6)	163 (5)	2.3
OW3	358 (7)	−1384 (7)	1678 (5)	2.7
OW4	−228 (6)	1343 (6)	−1794 (5)	2.2
OW5	3284 (8)	−1578 (11)	2874 (7)	5.2
OW6	−3235 (7)	1518 (8)	−2723 (5)	3.3

heat pump was used for cooling and a gold–chromel thermocouple with an accuracy of 0.1 K to measure the sample temperature. The balance was calibrated with CoHg(NCS)$_4$.[28] The sensitivity of the system was between 10^{-5}–10^{-6} emu, depending upon the field strength. Diamagnetic corrections for the constituent atoms were estimated by using Pascal's constants[29] and were as follows (cm^3·mol^{-1} × 10^6): 314.1 (MnXao), 315.1 (CoIno), 314.1 (CoXao), 306.2 (NiGuo), 310.7 (NiIno), 353.1 (NiXao), and 327.1 (CuXao).

Crystallographic Determination. The diffraction data were obtained at 20 °C by using a Nonius CAD-4 diffractometer. Unit cell parameters were refined from setting angles of 25 selected reflections ($12.89 < 2\theta < 21.49°$). The crystal data are listed in Table I and atomic coordinates are given in Table II; thermal parameters, as well as the tables of observed and calculated structure factors, are part of the supplementary material. The intensity data were corrected for Lorentz and polarization factors but not for absorption. The structure was solved by the heavy-atom method and refined by full-matrix least-squares techniques based on F. The H atoms were not located. The final refinement involved the x, y, z, and β_{ij} parameters of all the atoms. The maximum residual peak in the final ΔF map was 3.1 e·Å^3, located in an instertitial position. The computations were performed by means of the Enraf Nonius SDP system.[30]

(28) Bünzli, J. G. C. *Inorg. Chim. Acta* **1979**, *36*, L413.
(29) Mabbs, F. E.; Machin, D. J. *Magnetism and Transition Metal Complexes*; Chapman and Hall: London, 1973.
(30) *SDP Structure Determination Package*; B. A. Frenz & Associates Inc.: College Station, TX, 1982.

The compounds MnXao and CuXao have also been obtained in monocrystalline form, but their X-ray diffraction spots are too wide for their structure to be solved. Both compounds are monoclinic and have probable space groups $C2$ and $P2_1$ respectively. It was not possible to calculate the corresponding unit cell parameters with any great accuracy:

MnXao $a = 14.1$ Å, $b = 11.1$ Å, $c = 19.2$ Å, $\beta = 112°$

CuXao $a = 15.42$ Å, $b = 6.94$ Å, $c = 23.6$ Å, $\beta = 91.8°$

Results and Discussion

A series of divalent metal complexes with the anionic form of purine nucleosides has been obtained. During synthesis, we made every effort to avoid the formation of basic salts, which are readily generated, but the presence of small amounts of these may explain some of the small discrepancies in the elemental analysis data.

Thermal and Spectroscopic Studies. The dehydration of the complexes takes place in two steps, clearly to be seen in the TG and DSC diagrams as weight losses and endothermical effects. The first step takes place in the 60–90 °C temperature range, whereas the second occurs in the 120–170 °C range. The corresponding dehydration enthalpies are around 30 and 50 kJ·(mol of water)$^{-1}$. The weight loss associated with the second effect is in accordance with the expected value for four water molecules (two in the case of CdXao), whereas this value in the first step is the expected one for the remaining water molecules. This leads us to propose the distribution between coordinated and uncoordinated water as indicated in the nomenclature of the compounds. Pyrolytic decomposition begins at 220 °C and ends in the 500–700 °C range. The residues are identified as Mn$_2$O$_3$, Co$_3$O$_4$, NiO, CuO, ZnO, and CdO. We have published a more detailed thermal study of these complexes elsewhere.[31]

The most important feature in the infrared spectra of these compounds, when compared with the free ligands,[32] is the shift to lower frequencies of the band assigned to the stretching of carbonyl groups, which is typical of deprotonation processes of their neighboring endocyclic nitrogens. This seems to indicate that the nucleosides are in the anionic form and not in molecular form, which leads us to reject the possibility of tautomeric forms such as $[M(Nuc)_2(OH)_2(H_2O)_2]$. The displacement is very large (from 1700 to 1610 cm^{-1}) for the two inosine complexes; in all probability, not only deprotonation but also interaction with water molecules is responsible for this shift. Otherwise, in xanthosine complexes, the single $\nu(C{=}O)$ band of the free ligand at 1682 cm^{-1} is split into two signals, one of them at almost the same frequency and another displaced downwards to 1660–1640 cm^{-1}, attributable to C6=O and C2=O, respectively. The presence of guanosine $\delta(NH_2)$ in the NiGuo spectrum makes an assignment for this compound uncertain. Absorptions of skeletal stretching vibrations ($\nu(C{=}C) + \nu(C{=}N)$) show random variation when compared with the spectra of the nucleosides.

The presence of a broad intense absorption in the 2800–3600-cm^{-1} region ($\nu(O{-}H)$ of sugar and water) prevented us from observing any possible variation in the $\nu(N{-}H)$ bands. Signals due to $\nu(M{-}O)$ or $\nu(M{-}N)$ vibration modes were not clearly identified, whereas bands assigned to $\nu(C{-}O)$ of the ribose unit do not change appreciably on the formation of the complexes.

The only compound for which the ^{1}H and ^{13}C NMR spectra could be recorded was CdXao (ZnXao is very poorly soluble in DMSO whereas the remaining compounds are paramagnetic). The proton spectrum shows signals at 10.16 (s, N1-H), 7.78 (s, C8-H), 5.72 (d, C1′-H), 4.45 (t, C2′-H), 4.08 (t, C3′-H), 3.95 (c, C4′-H), 3.63 (dd, C5′-H pro S), and 3.53 ppm (dd, C5′-H pro R). If a comparison with free xanthosine is made, we can see that N1-H and C8-H are shielded by 0.7 and 0.1 ppm, respectively. Nevertheless, the most significant changes occur in the signals of the two diasterotopic hydrogens in the 5′-position; these signals appear in adenosine, guanosine, and inosine separately as two double doublets, whereas in xanthosine they are superimposed as one single doublet as though they were equivalent, which

(31) Quirós, M.; Sánchez, M. P.; Romero, M. A.; Salas, J. M. *Thermochim. Acta* **1988**, *133*, 335.
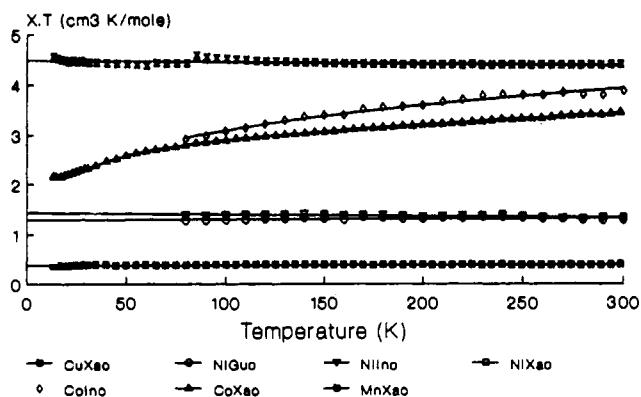(32) Tselepi-Kalouli, E.; Katsaros, N. *J. Inorg. Biochem.* **1988**, *34*, 63.

Figure 1. Magnetic data for the paramagnetic compounds described in this paper, represented as χT versus T.

Table III. Magnetic Data for the Nucleosidate Complexes

compound	μ_{eff},[a] μ_B	C, emu/(mol·K)	θ, K	μ,[b] μ_B
MnXao	5.91	4.306 ± 0.008	-4.0 ± 0.4	5.87 ± 0.01
CoIno	5.54	4.41 ± 0.03	43.5 ± 2.3	5.94 ± 0.02
CoXao	5.24	3.74 ± 0.04	31.7 ± 2.4	5.47 ± 0.03
NiGuo	3.20	1.31 ± 0.01	-0.5 ± 1.7	3.24 ± 0.02
NiIno	3.23	1.29 ± 0.01	-10.2 ± 2.2	3.21 ● 0.02
NiXao	3.27	1.31 ± 0.01	-7.8 ± 1.1	3.23 ± 0.02
CuXao	1.75	0.387 ± 0.001	1.3 ± 0.3	1.76 ± 0.01

[a] At 298.7 K. [b] From C.

we attribute to the existence of an N3–H···O5′ intramolecular hydrogen bond, which forces a syn conformation and changes the environment of the C5′ hydrogens. In the CdXao spectrum, the two protons appear separately, as they do in the anti-conformed nucleosides; this could be due to the presence of the metal atom coordinated to the nitrogen in the 3-position, which would induce the glycosidic conformation to alter from syn to anti. The small displacement of the C8–H resonance seems also to eliminate the possibility of the imidazole ring as being the coordination place since this would generate a higher shift.[22]

Moreover, the ^{13}C NMR spectrum strongly supports this idea. It shows signals at 159.00 (C2), 158.19 (C6), 150.24 (C4), 135.41 (C8), 115.42 (C5), 87.65 (C1′), 86.08 (C4′), 73.64 (C2′), 70.81 (C3′), and 61.81 ppm (C5′). Very large deshieldings are observed for C2 (8.52 ppm) and C4 (10.87 ppm), whereas the displacements for the remaining signals are below 1 ppm.

It must be pointed out that these data do not agree with the crystallographic results for ZnXao (see below), which indicate N7 coordination, although with ZnXao we are dealing with a solid-state structure and with CdXao with a solution structure. Dissolving CdXao in DMSO should introduce modifications into the coordination sphere of cadmium, with the solvent probably entering. Unfortunately we have not been able to obtain CdXao in monocrystalline form.

Magnetic Properties. The magnetic measurements for the nucleosidate complexes are set out in Figure 1, where the product χT (proportional to μ^2) is plotted versus the temperature.

It can be seen that the effective magnetic moments for the manganese, nickel, and copper complexes are almost constant within our experimental temperature range. This is supported by the low values for the θ parameter of the Curie–Weiss law [obtained by adjusting $1/\chi$ vs T by least-squares methods (Table III)]. The values of μ_{eff} at room temperature (very similar to those obtained from Curie's constants) are consistent with high-spin compounds in which the metal ion lies in an octahedral crystal field.[33]

The corresponding curves for the two cobalt complexes (CoIno and CoXao) show a decrease in the effective moment concomitant
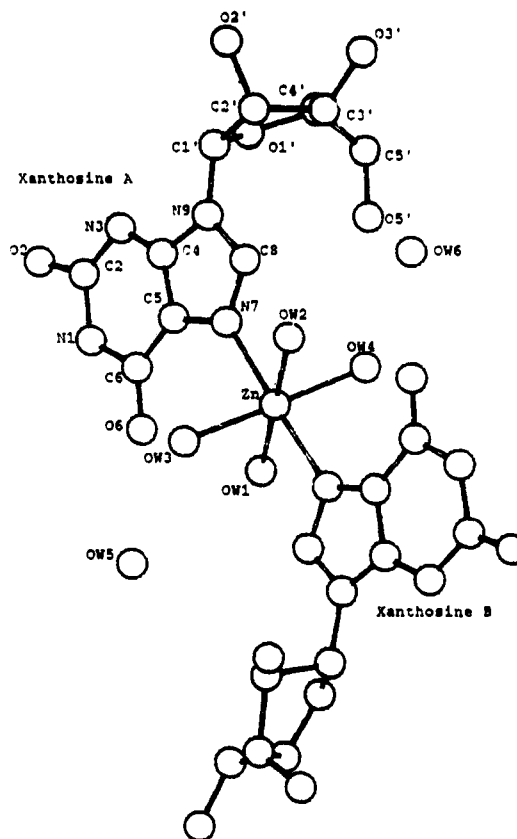

Figure 2. View of the ZnXao structure.

with temperature, its value varying from 5.24 to 4.15 μ_B (CoXao) and from 5.54 to 4.88 μ_B (CoIno). This dependence is typical of octahedrally coordinated high-spin Co(II) compounds,[33] as well as the high θ values, and is not attributable to the existence of antiferromagnetic interactions. The μ_{eff} values at room temperature clearly suggest the presence of an appreciable orbital contribution (spin-only value is about 3.9 μ_B for Co(II)), which completely rules out the possibility of a tetrahedral coordination; the value for CoXao is within the normal range for octahedral Co(II) whereas that for CoIno is somewhat high.

Description of the Structure of ZnXao. The crystal structure consists of discrete $[Zn(Xao)_2(H_2O)_4]$ units plus two additional water molecules at interstitial positions (Figure 2). The metal atom is surrounded octahedrally by four water molecules lying in the equatorial plane and two N7-coordinated xanthosinate anions at the apexes. The zinc atom acts as a quasi-symmetry center for the water and purine atoms (obviously not for the chiral ribose moieties). The structurally nearest compounds we have found are the two formed by Zn(II) with the methyl ester derivatives of the nucleotides GMP and IMP,[34] the formulas of which are also $[ZnL_2(H_2O)_4]$ with N(7)-coordinated nucleotides, although they are cis-disposed. Bond distances and angles are included in Table IV.

The distortion of the octahedron around Zn is not very severe; the distances Zn–OW are very close to those in the above-mentioned compounds[34] and are in the usual range for such distances.[35,36] The distances Zn–O are in the same range for both aquo and hydroxyl complexes,[37,38] which prevents us from distinguishing these two situations with these data alone.

The most acidic proton in free xanthosine is the one attached to N3,[22] so we should expect that this is the one lost in the for-

(33) Casey, A. T.; Mitra, S. *Theory and Applications of Molecular Paramagnetism*; Boudreaux, E. A., Mulay, L. N., Eds.; Wiley: New York, 1976.

(34) Miller, S. K.; VanDerveer, D. G.; Marzilli, L. G. *J. Am. Chem. Soc.* **1985**, *107*, 1048.

(35) Follner, H.; Brehler, B. *Acta Crystallogr.* **1968**, *24B*, 1339.

(36) Van Niekerk, J. N.; Schoening, F. R. L.; Talbot, J. H. *Acta Crystallogr.* **1953**, *6*, 720.

(37) Allman, R. *Z. Kristallogr.* **1968**, *126*, 417.

(38) Merrit, L.; Cady, R. T.; Mundy, B. W. *Acta Crystallogr.* **1954**, *7*, 473.

Table IV: Bond Distances (Å) and Angles (deg), Distances between Hydrogen-Bonded Atoms (Å), and Selected Torsion Angles (deg) in [Zn(Xao)₂(H₂O)₄]·2H₂O

Bond Distances

Zn-OW1	2.113 (5)	Zn-OW2	2.078 (5)	Zn-OW3	2.070 (5)	Zn-OW4	2.150 (5)

	xanthosine A	xanthosine B		xanthosine A	xanthosine B
Zn-N7	2.166 (6)	2.186 (6)	C8-N9	1.397 (9)	1.341 (8)
N1-C2	1.392 (9)	1.404 (10)	N9-C1'	1.431 (10)	1.491 (9)
N1-C6	1.383 (7)	1.366 (9)	C1'-O1'	1.414 (8)	1.379 (7)
C2-O2	1.297 (8)	1.227 (8)	C1'-C2'	1.541 (9)	1.511 (9)
C2-N3	1.324 (8)	1.363 (8)	O1'-C4'	1.442 (10)	1.446 (9)
N3-C4	1.342 (8)	1.361 (8)	C2'-O2'	1.440 (10)	1.402 (8)
C4-C5	1.363 (10)	1.390 (9)	C2'-C3'	1.501 (10)	1.553 (10)
C4-N9	1.388 (8)	1.352 (7)	C3'-O3'	1.435 (9)	1.404 (10)
C5-C6	1.389 (8)	1.470 (9)	C3'-C4'	1.552 (10)	1.536 (9)
C5-N7	1.464 (8)	1.336 (7)	C4'-C5'	1.491 (14)	1.523 (10)
C6-O6	1.240 (8)	1.241 (10)	C5'-O5'	1.443 (12)	1.434 (10)
N7-C8	1.330 (10)	1.297 (8)			

Bond Angles

OW1-Zn-OW2	178.7 (2)	OW2-Zn-OW3	95.5 (2)	OW3-Zn-OW4	176.2 (2)
OW1-Zn-OW3	85.3 (2)	OW2-Zn-OW4	87.4 (2)	N7A-Zn-N7B	177.9 (2)
OW1-Zn-OW4	91.8 (2)				

	xanthosine A	xanthosine B		xanthosine A	xanthosine B
N7-Zn-OW1	93.9 (2)	86.9 (2)	C5-N7-C8	104.0 (6)	106.4 (5)
N7-Zn-OW2	85.1 (2)	94.2 (2)	N7-C8-N9	112.4 (5)	111.6 (5)
N7-Zn-OW3	92.9 (2)	89.1 (2)	C4-N9-C8	106.7 (5)	107.6 (5)
N7-Zn-OW4	84.9 (2)	93.1 (2)	C4-N9-C1'	122.9 (5)	122.5 (5)
C2-N1-C6	126.5 (5)	126.8 (6)	C8-N9-C1'	130.3 (5)	129.0 (5)
N1-C2-O2	114.9 (6)	119.9 (6)	N9-C1'-O1'	109.6 (6)	109.2 (5)
N1-C2-N3	121.7 (5)	119.5 (5)	N9-C1'-C2'	115.2 (6)	112.8 (5)
O2-C2-N3	123.4 (6)	120.5 (7)	O1'-C1'-C2'	105.6 (5)	104.9 (5)
C2-N3-C4	111.6 (6)	115.3 (6)	C1'-O1'-C4'	112.4 (5)	107.2 (5)
N3-C4-C5	129.5 (6)	128.2 (5)	C1'-C2'-O2'	104.2 (6)	115.2 (5)
N3-C4-N9	122.8 (6)	127.2 (6)	C1'-C2'-C3'	102.9 (5)	98.6 (5)
C5-C4-N9	107.6 (5)	104.5 (5)	O2'-C2'-C3'	111.1 (7)	115.5 (6)
C4-C5-C6	120.1 (6)	116.0 (5)	C2'-C3'-O3'	112.6 (6)	108.7 (5)
C4-C5-N7	109.3 (5)	109.8 (5)	C2'-C3'-C4'	104.8 (6)	101.4 (6)
C6-C5-N7	130.6 (6)	134.1 (6)	O3'-C3'-C4'	109.9 (6)	110.5 (6)
N1-C6-C5	110.3 (6)	113.9 (6)	O1'-C4'-C3'	104.8 (6)	106.6 (5)
N1-C6-O6	119.8 (5)	120.3 (6)	O1'-C4'-C5'	111.1 (8)	106.0 (6)
C5-C6-O6	129.8 (5)	125.7 (6)	C3'-C4'-C5'	117.0 (8)	114.6 (6)
Zn-N7-C5	132.6 (5)	133.7 (4)	C4'-C5'-O5'	110.1 (9)	111.0 (7)
Zn-N7-C8	123.3 (4)	119.7 (4)			

Hydrogen Bonding Distances

N1A···O6B (x + 1, y - 1, z)	2.798 (7)	OW5···O2B (x + 1, y - 1, z)	2.788 (9)
N1B···O6A (x - 1, y + 1, z)	2.771 (8)	OW3···N3B (x, y - 1, z)	2.810 (8)
OW1···O6A (x, y, z)	2.658 (7)	O2'B···O1'A (x, y + 1, z + 1)	2.797 (8)
OW2···O6B (x, y, z)	2.730 (7)	O2'A···O3'B (x - 1, y - 1, z - 1)	2.771 (9)
OW1···O2A (x, y + 1, z)	2.697 (8)	O5'B···O2'B (x + 1, y, z)	2.798 (8)
OW6···O2A (x - 1, y + 1, z)	2.728 (8)	OW6···O5'B (x - 1, y, z - 1)	2.859 (9)
OW4···N3A (x, y + 1, z)	2.769 (7)	OW3···OW5 (x, y, z)	2.786 (9)
OW2···O2B (x, y - 1, z)	2.704 (7)	OW4···OW6 (x, y, z)	2.699 (8)

Torsion Angles

	xanthosine A	xanthosine B		xanthosine A	xanthosine B
C8-N9-C1'-O1' (Φ_{CN})	99.8 (8)	47.5 (8)	O1'-C4'-C3'-C2' (N_3)	-19.5 (7)	14.9 (7)
C8-N9-C1'-C2'	-18.9 (9)	-68.6 (8)	C1'-O1'-C4'-C3' (N_4)	0.6 (8)	14.3 (7)
C2'-C1'-O1'-C4' (N_0)	18.1 (8)	-39.0 (7)	O5'-C5'-C4'-O1' (Φ_{OO})	-70.2 (9)	170.8 (6)
O1'-C1'-C2'-C3' (N_1)	-29.4 (7)	46.6 (6)	O5'-C5'-C4'-C3' (Φ_{CO})	50.1 (8)	-71.9 (8)
C1'-C2'-C3'-C4' (N_2)	29.4 (7)	-35.4 (6)			

mation of the xanthosinato anion. The other possibility (N1-H) can be ruled out due to the existence of N1-H → O6 intermolecular contacts. The resulting negative charge must be very spread out across the purine rings with the water molecules also probably supporting part of it. In xanthosine A, the C2-O2 bond is longer and the C2-N3 shorter in comparison with those in free xanthosine;[39,40] surprisingly, these changes are not observed in xanthosine B. Nevertheless, we must emphasize that standard deviations in distances and angles may be underestimated due to the presence of the pseudosymmetry center. The changes in the angles N1-C2-N3, C2-N3-C4, and N3-C4-C5 (the second is closed and the other two are open, compared to free xanthosine), similar to those in sodium xanthinate,[41] are probably more sig-

nificant, supporting the idea of N3 deprotonation rather than the presence of hydroxyl groups.

Both purine rings are flat with the endocyclic atoms deviating less than 0.03 Å out of the average planes, which are almost perpendicular to the equatorial (Zn-OW1-OW2-OW3-OW4) plane, the dihedral angles with the Zn-N7A-N7B-OW1-OW2 and Zn-N7A-N7B-OW3-OW4 planes being about 30 and 60°, respectively.

Contacts assigned as being hydrogen bonds are also summarized in Table IV. Some of them are particularly important, such as OW1 → O6A and OW2 → O6B, which form two seven-member (including the hydrogen) pseudochelate rings around the metal atom and probably stabilize the complex. Such an interaction has been also observed in the Co(III) complexes with IMP and

(39) Koyama, G.; Nakamura, N.; Umezawa, H.; Iitaka, Y. *Acta Crystallogr.* **1976**, *B32*, 969.

(40) Lesyng, B.; Marck, C.; Saenger, W. *Z. Naturforsch.* **1984**, *39C*, 720.

(41) Mizuno, H.; Fujiwara, T.; Tomita, K. *Bull. Chem. Soc. Jpn.* **1969**, *42*, 3099.

GMP.[42] The pair of interactions N1A → O6B and N1B → O6A, which is very similar to the hydrogen bonds between complementary bases in the two chains that form DNA, are also noteworthy (structure I). Bonds attaching O2 and N3 to water

I
hydrogen bonding in which
purine atoms are involved
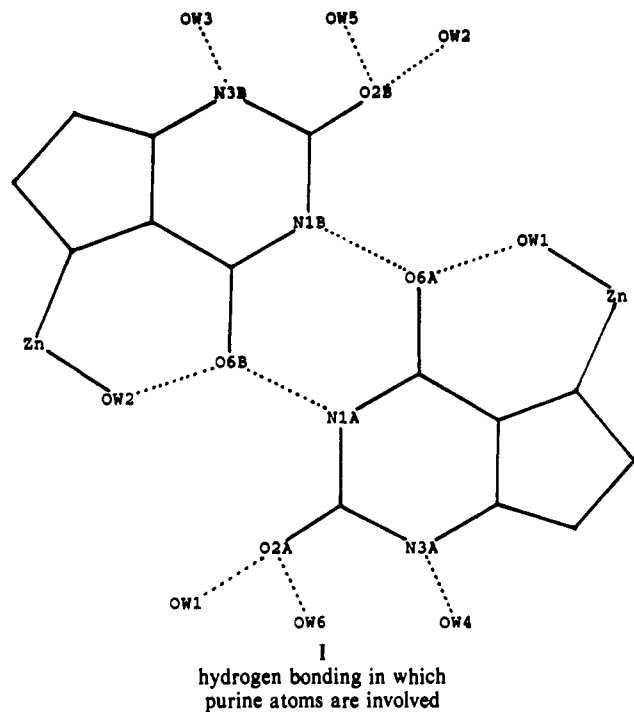
(42) Poojary, M. D.; Monohar, H. *J. Chem. Soc., Chem. Commun.* **1982**, 533.

molecules certainly help in the distribution of the negative charge. No purine stacking is to be seen, as is the case with the zinc complexes of the GMP and IMP derivatives.[34]

Ribose A is C2′-exo puckered, whereas ribose B is somewhat irregular, more like C3′-exo; the most usual ribose puckerings are C2′-endo and C3′-endo. Furthermore, the configuration around C4′–C5′ is gauche–gauche for ribose A and trans–gauche for ribose B, the last one being much less frequent than the usual gauche–gauche and gauche–trans.

Finally, we must mention that the values of R and R_w are slightly high. This might be due to the fact that we were unable to locate the hydrogen atoms (about 9% of the electron density) and perhaps to small problems in the refinement process caused by the pseudosymmetry.

Registry No. MnXao, 133986-23-9; CoIno, 133986-24-0; CoXao, 133986-25-1; NiGuo, 133986-26-2; NiIno, 133986-27-3; NiXao, 133986-30-8; CuXao, 133986-28-4; ZnXao, 133986-29-5; CdXao, 133986-31-9.

Supplementary Material Available: Table S-1 (anisotropic temperature factors), Table S-2 (angles between atoms involved in hydrogen bonding), and Table S-3 (plane calculations) (3 pages); Table S-4 (observed and calculated structure factors) (37 pages). Ordering information is given on any current masthead page.

Contribution from the Department of Chemistry, Stanford University, Stanford, California 94305, and Division of Chemistry and Chemical Engineering, California Institute of Technology, Pasadena, California 91125

Electronic Effects of Bis(acetylacetone) in Ruthenium(II) and Ruthenium(III) Complexes

Tai Hasegawa,[†] T. C. Lau,[†] H. Taube,*,[†] and W. P. Schaefer[‡]

The compound Ph₄As[Ru(acac)₂Cl₂] was prepared by the reaction of RuCl₃·3H₂O with acetylacetone in 1 M aqueous KCl. The anion was shown by X-ray crystallography to have a trans configuration, and it is the first *trans*-bis(acetylacetone) complex to have been prepared. The compound crystallizes in the monoclinic system, in the space group $P\bar{1}$, with $a = 10.082$ (2) Å, $b = 13.433$ (2) Å, $c = 14.950$ (2) Å, $\alpha = 65.03$ (1)°, $\beta = 66.71$ (1)°, $\gamma = 72.02$ (2)°, $V = 1663$ (1) Å³, and $Z = 2$. A number of *trans*-(acac)₂ complexes of ruthenium(II), -(III), and -(IV) were prepared from the above compound and were characterized by IR, UV–vis, and ¹H NMR spectroscopy and by cyclic voltammetry. They include *trans*-[Ru(acac)₂(pyrazine)₂] and *trans*-[Ru(acac)₂(CH₃CN)₂]. The analogous cis complexes were prepared by the reaction of the ligands pyrazine and CH₃CN with Ru(acac)₃ or by thermoisomerization of the trans species, and a comparison of chemical behavior was made. For the acetonitrile derivative, the equilibrium quotient for the isomerization of the trans species to the cis was measured as 80 at 30 °C. Isomerization is so slow for the pyrazine derivative compared to the competing decomposition that a dependable value of the equilibrium quotient could not be determined, but the indications are that the cis form is the more stable. These results, and measurements of the proton affinities of the pyrazine complexes, are rationalized on the basis that when two π-acid ligands compete for π-electron density, this competition is less severe when they are disposed cis, rather than trans, to each other. None of the observations suggest that acac⁻ acts significantly in a π-acid capacity. When Ru(acac)₂(CH₃OH)₂ and pyrazine, mixed in equimolar proportions, react, a very insoluble polymeric material forms. The solid is a poor conductor, but the conductance is increased by a factor as high as 10⁶ when it is doped with I₂.

Ligands of the acetylacetone type have played an important role in the development and practice of coordination chemistry.[1] Despite this, little systematic work has been done on the influence it has, acting as a coligand, on the reactivity and properties of

a test ligand in a complex. The ligand as the anion is potentially a σ donor, a π donor, and a π acceptor. In undertaking the work to be described, we were particularly interested in the net effect of the three possible modes of interaction and chose for this purpose

---

[†] Stanford University.
[‡] California Institute of Technology.

(1) Mehrotra, R. C.; Bohra, R.; Gaur, D. P. *Metal β-Diketonates and Allied Derivatives*; Academic Press: New York, 1978.